Electronic Supplementary Information

Insights into the Polymorphic Transformation Mechanism of Aluminum Hydroxide during Carbonation of Potassium aluminate Solution

You-Fa Jiang, Cheng-Lin Liu, Jin Xue, Ping Li, Jian-Guo Yu**

National Engineering Research Center for Integrated Utilization of Salt Lake Resource, State Key Laboratory of Chemical Engineering, East China University of Science and Technology, Shanghai, China.

Table of contents **Page**

* Tel./fax: +86-021-64252170. E-mail: (C.L.) liuchenglin@ecust.edu.cn. E-mail: (J.Y.) jgyu@ecust.edu.cn.

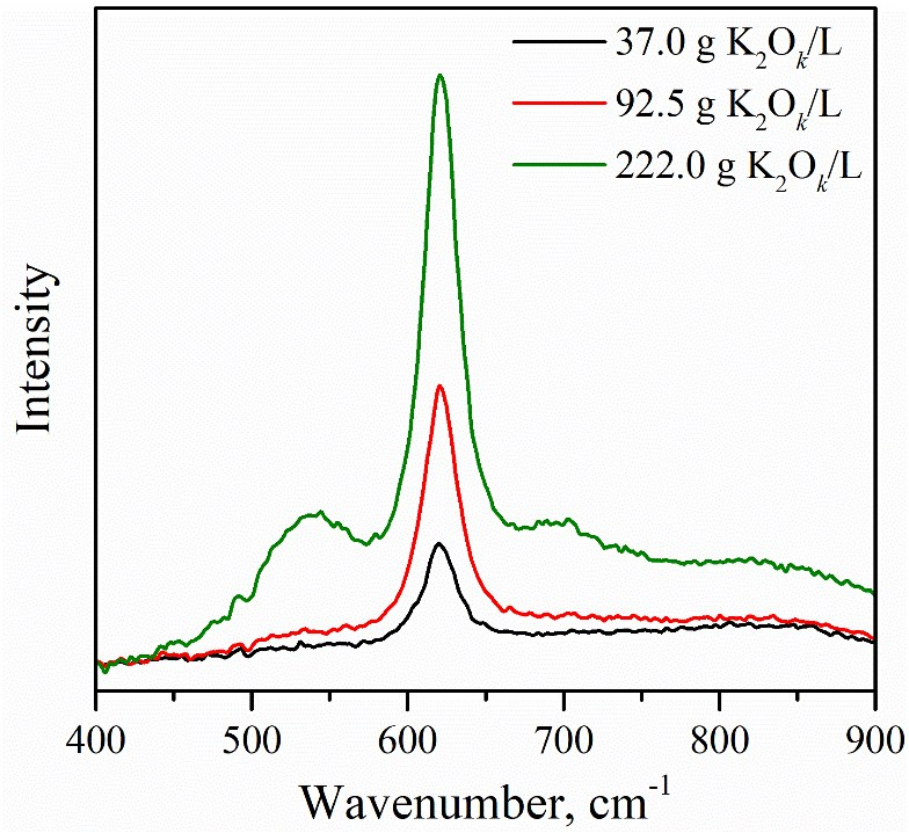

Fig. S1 Raman spectra of potassium aluminate solutions at room temperature.

Raman spectra of pregnant liquors in the region of interest (400-900 cm^{-1}) is shown in Fig. S1. The pregnant liquors of three different concentrations adopted in this work appears to exhibit different constituents especially for the concentrated solutions. One significant band centred on ~620 cm^{-1} is present ignorance of the solution concentration, which is assigned to the symmetric ν_1-AlO_4 stretching of the pseudotetrahedral $Al(OH)_4^-$.[1] As the solution concentration reaches 222.0 g K_2O_k/L (Bayer conditions), two new modes emerge on both sides of the $Al(OH)_4^-$ bonds. It is widely accepted that the sidebands are attributed to the formation of oxygen-bridged dimer:[2]

$$2Al(OH)_4^- \rightleftharpoons (OH)_3Al - O - Al(OH)_3^{2-} + H_2O$$

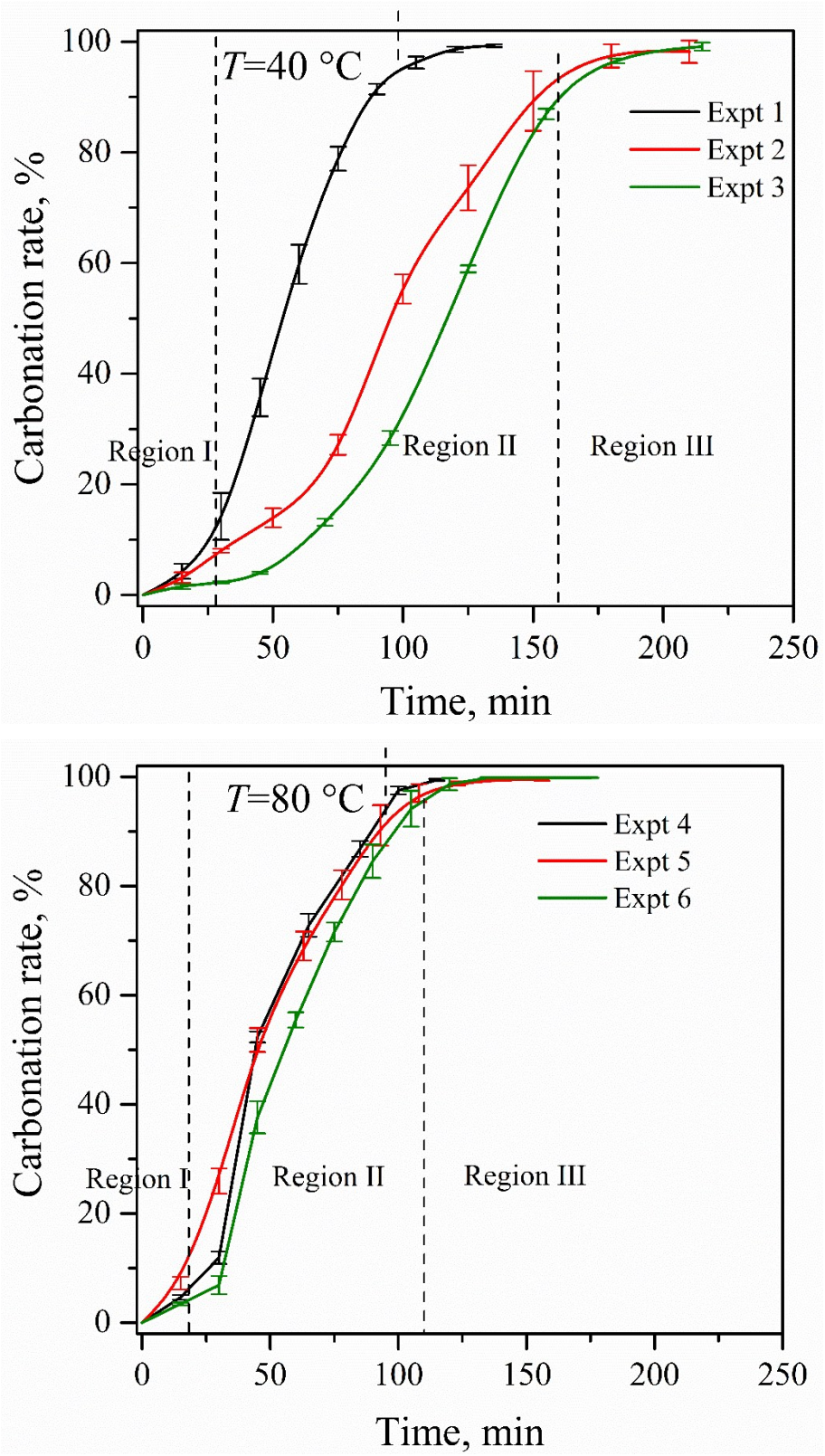

Fig. S2. Carbonation rate of potassium aluminate solution carbonated under Expt 1~6.

The representative plots of carbonation rate versus time, presented in Fig. S2, show three distinct regions. In region I, the carbonation rate increases slowly with time especially for experiments at 40 °C. This result indicates the dominant reaction between

the free hydroxide ions and added protons originated from the water-soluble reaction of CO_2 in the early stage of decomposition. In region II, a linear relationship between carbonation rate and time with a sharp slope is present. Owing to the continuous introduction of CO_2, a high level of supersaturation is maintained during the carbonation process. The majority of alumina in solutions is precipitated according to the following reactions:

$$Al(OH)_4^-(aq) \rightleftharpoons Al(OH)_3(s) + OH^-(aq)$$

$$OH^-(aq) + H^+(aq) \rightleftharpoons H_2O$$

In region III, the carbonation rate approaches approximately 100% and slows down.

Table S1. The sampling time for initial crystalline product and final product under different experimental conditions

Experimental condition		Expt 1	Expt 2	Expt 3	Expt 4	Expt 5	Expt 6	Expt 7	Expt 8	Expt 9
Sampling time, min	Initial crystalline product	15	15	15	15	15	15	30	30	15
	Final product	135	210	215	115	155	175	120	185	230

Table S2. The relative fractional amount of bayerite and gibbsite during carbonation of potassium aluminate solutions

Experimental condition		Expt 1	Expt 2	Expt 3	Expt 4	Expt 5	Expt 6	Expt 7	Expt 8	Expt 9
Initial crystalline product	Bayerite	1	1	1	1	1	1	0.52	0.81	0.54
	Gibbsite	0	0	0	0	0	0	0.48	0.19	0.46
Final product	Bayerite	1	0.81	0.39	0.63	0.01	0.02	0..07	0.11	0.09
	Gibbsite	0	0.19	0.61	0.37	0.99	0.98	0.93	0.89	0.91

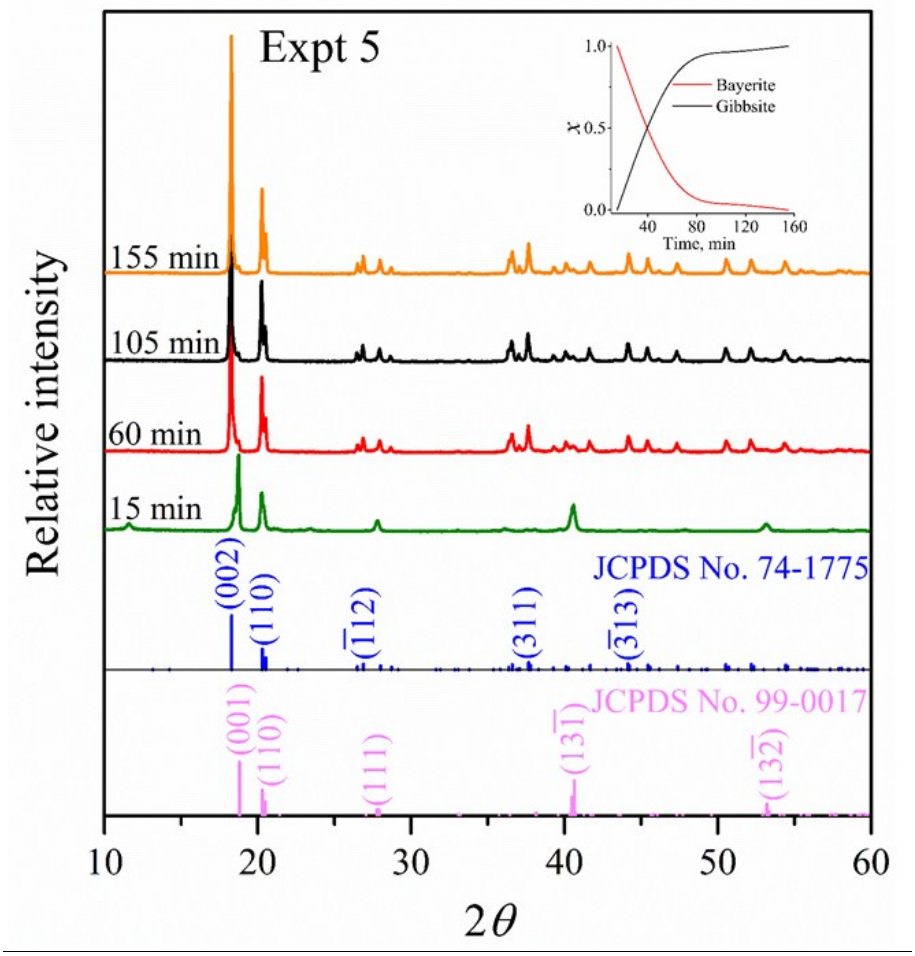

Fig. S3. The representative XRD patterns of precipitates obtained in different sampling time. The smaller coordinate illustrate the variation of quantitative ratio of the polymorphs versus time. The calculated relative quantitative ratio of the polymorphs content indicates an equilibrium when the final product was sampled.

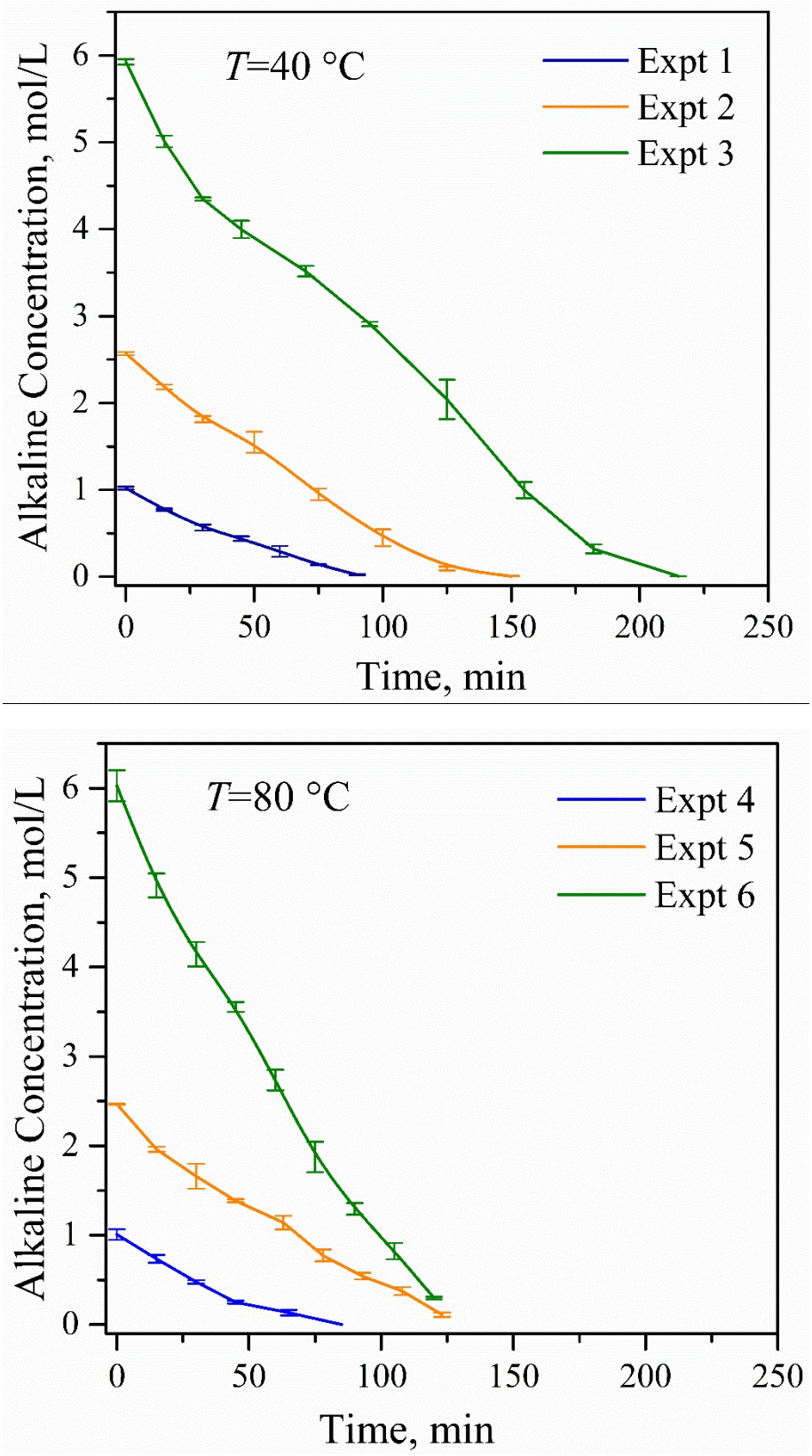

Fig. S4. Variation of alkaline concentration during carbonation process under Expt 1~6.

Calculation of supersaturation ratio (*S*):

$$S = \frac{S_X}{C_{Solution}},$$

$$S_X = K_{sp,\,X}(T) \times [OH^-], \text{ mol/L}$$

where S denotes the supersaturation ratio, S_X the saturation concentration, X gibbsite or bayerite, $C_{Solution}$ the solution concentration, $K_{sp,\,X}(T)$ the solubility product and $[OH^-]$ the alkaline concentration.

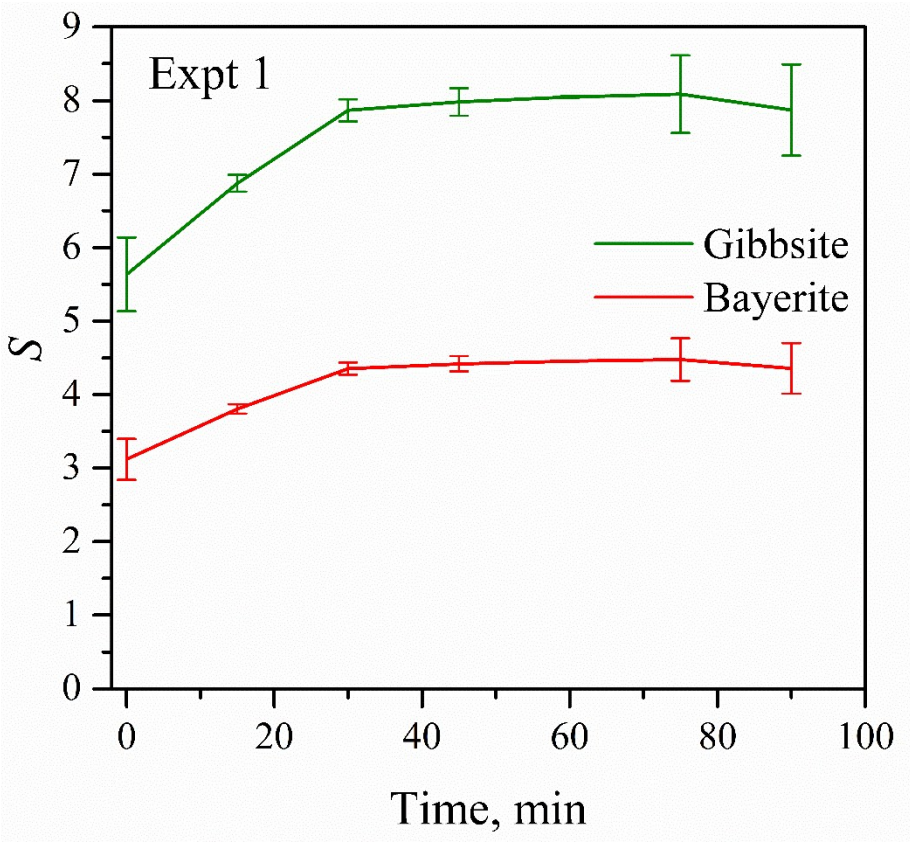
Expt 1
Gibbsite
Bayerite
S
Time, min
0
1
2
3
4
5
6
7
8
9
0
20
40
60
80
100

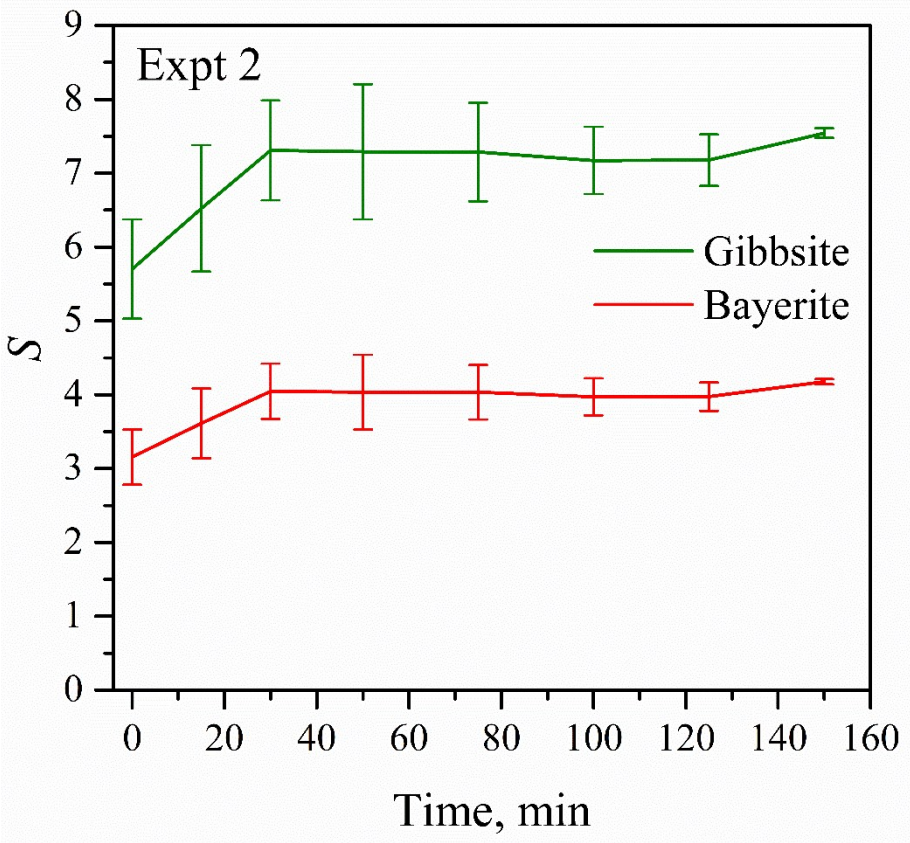
Expt 2
Gibbsite
Bayerite
S
Time, min
0
1
2
3
4
5
6
7
8
9
0
20
40
60
80
100
120
140
160

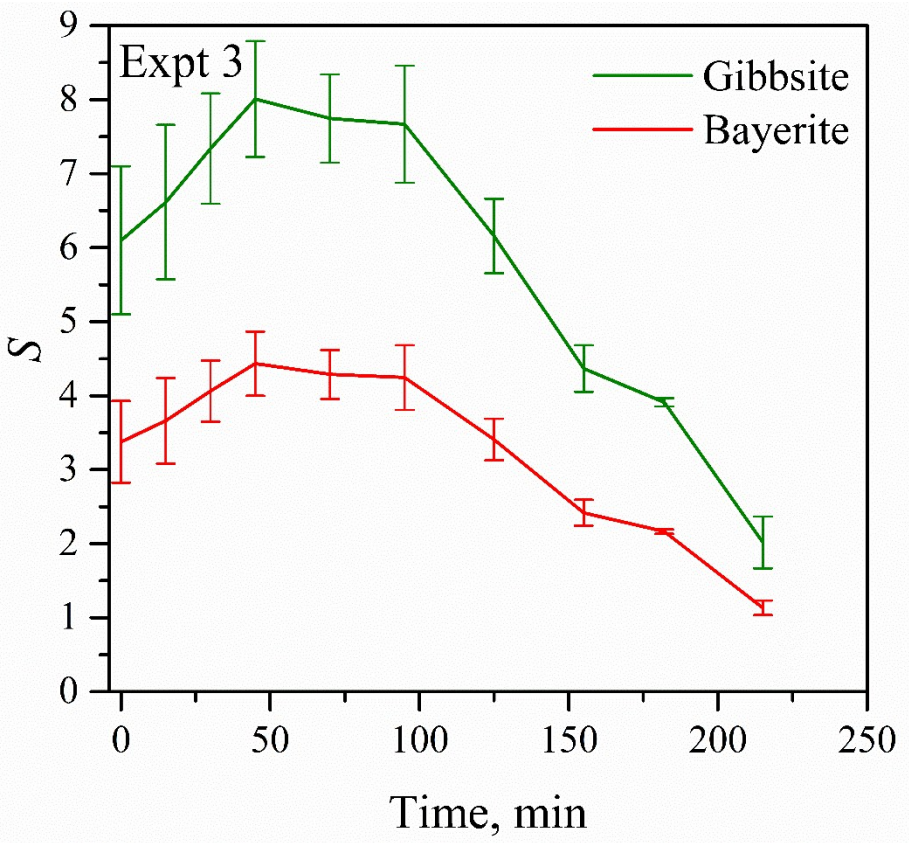
Expt 3
Gibbsite
Bayerite
S
Time, min
0
1
2
3
4
5
6
7
8
9
0
50
100
150
200
250

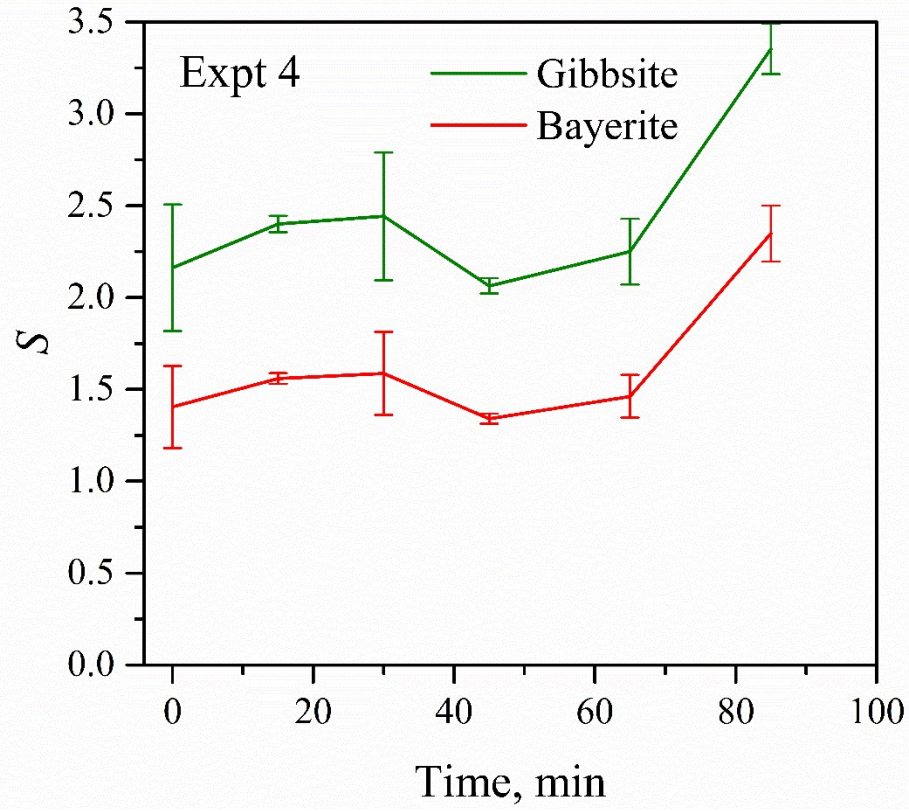
Expt 4
Gibbsite
Bayerite
S
Time, min
0.0
0.5
1.0
1.5
2.0
2.5
3.0
3.5
0
20
40
60
80
100

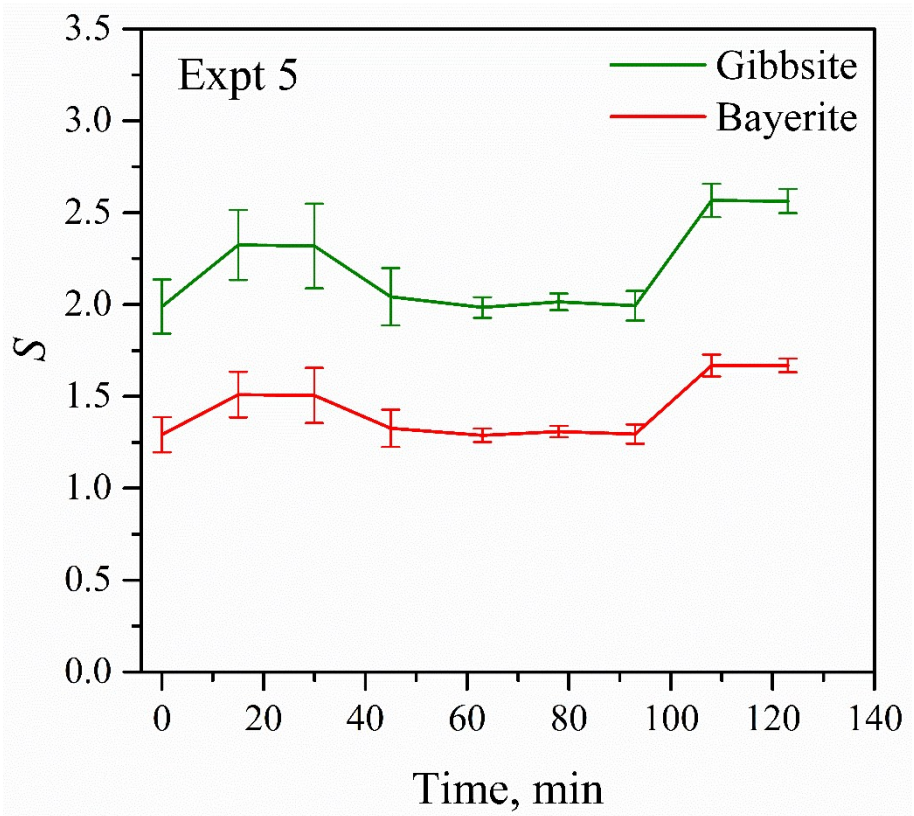

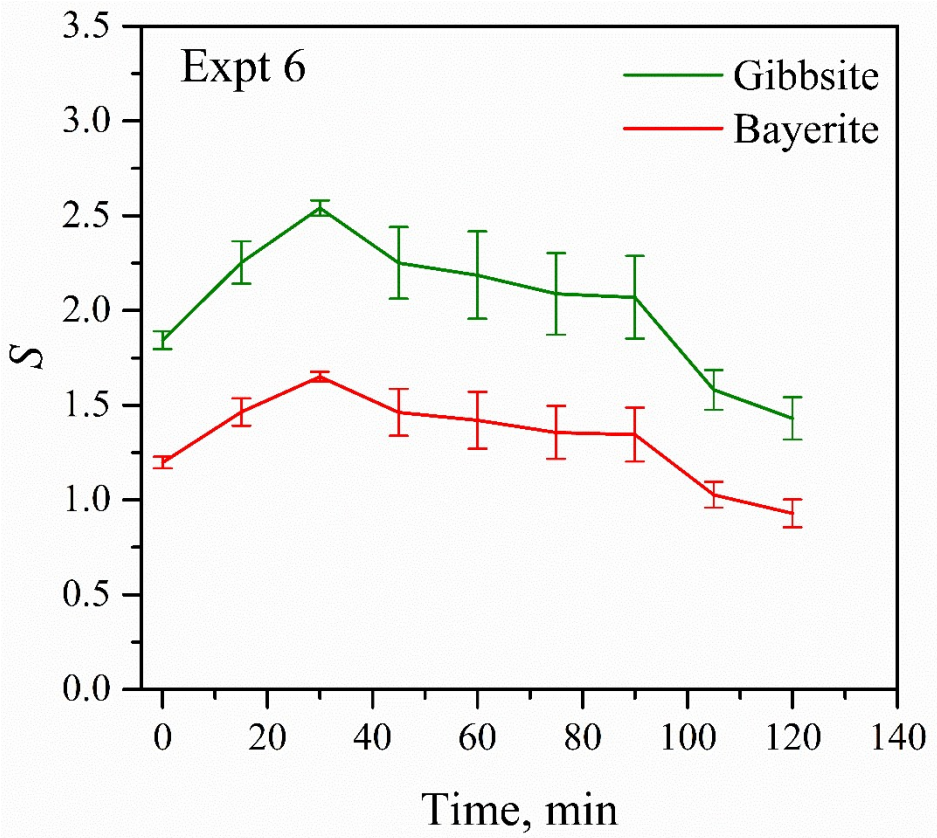

Fig. S5. Variation of supersaturation ratio during carbonation process under Expt 1~6.

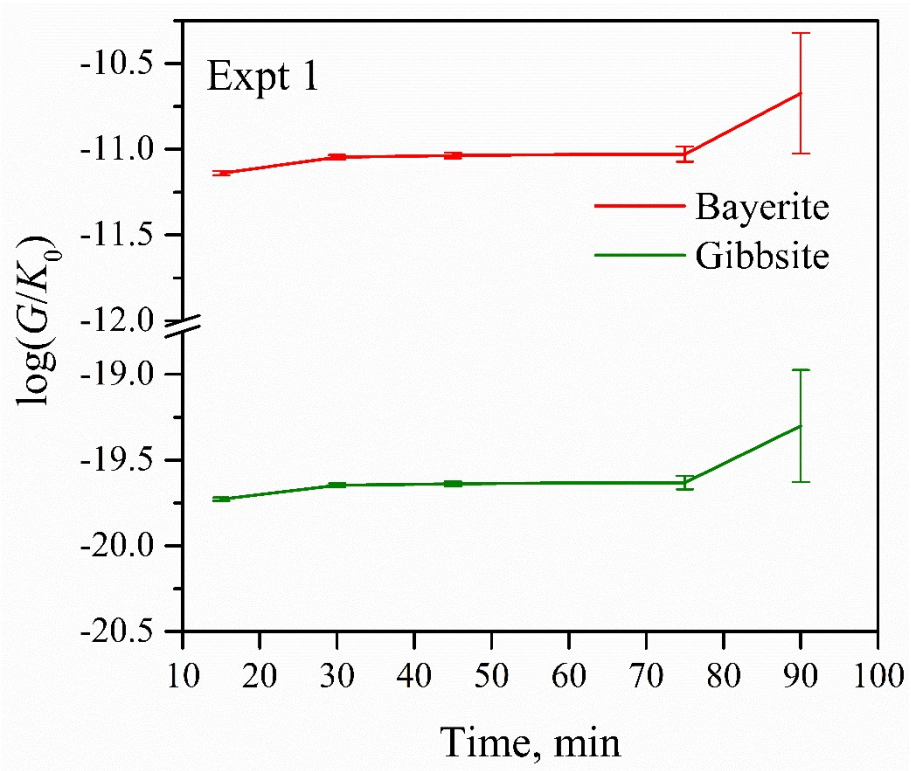
Expt 1
Bayerite
Gibbsite
log(G/K0)
-10.5
-11.0
-11.5
-12.0
-19.0
-19.5
-20.0
-20.5
10
20
30
40
50
60
70
80
90
100
Time, min

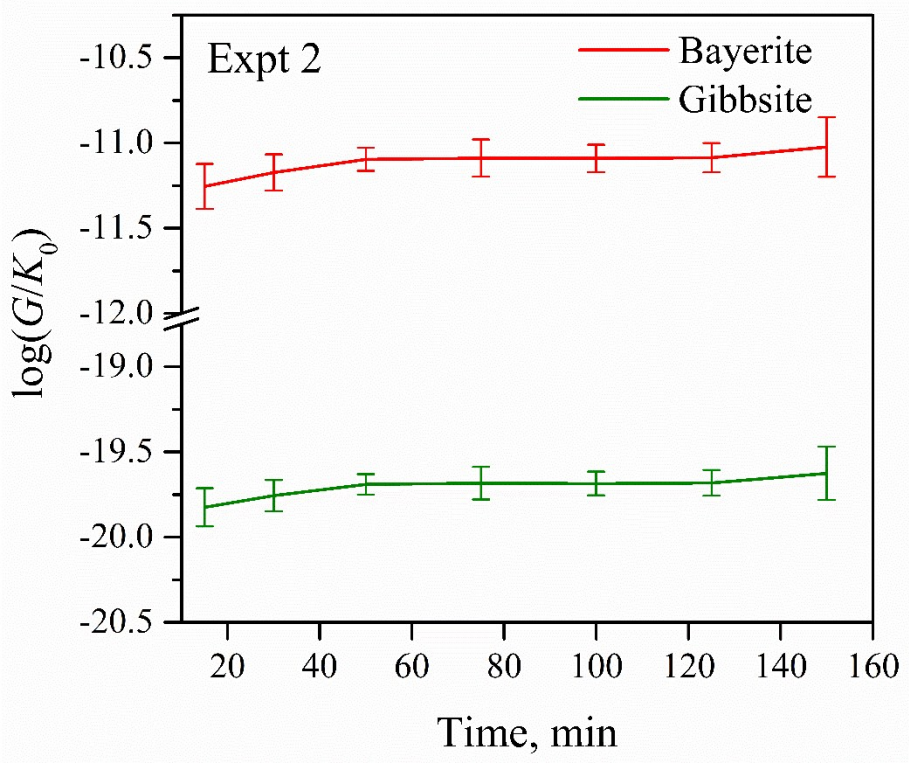
Expt 2
Bayerite
Gibbsite
log(G/K0)
-10.5
-11.0
-11.5
-12.0
-19.0
-19.5
-20.0
-20.5
20
40
60
80
100
120
140
160
Time, min

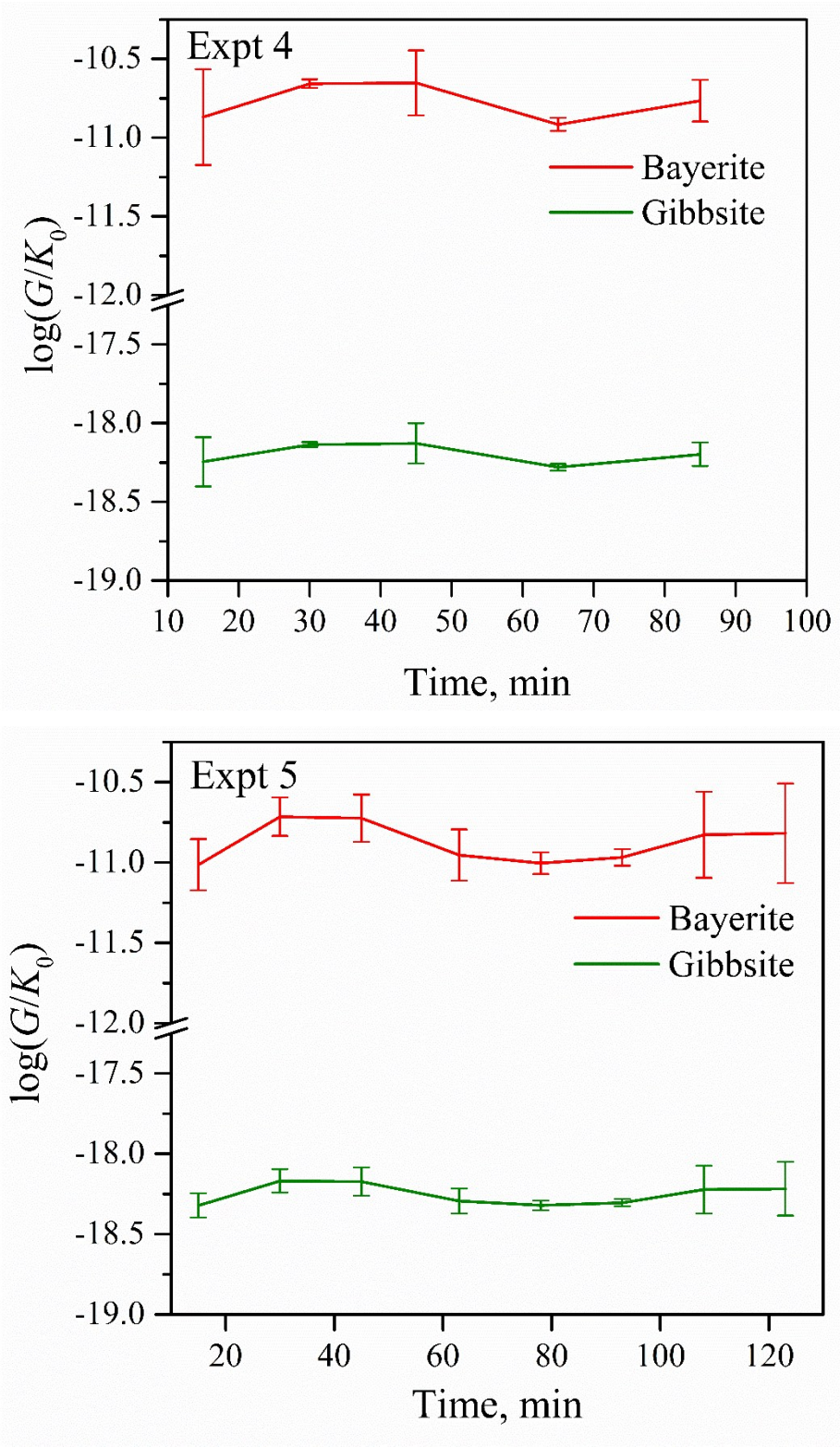

Fig. S6. Growth rate of gibbsite and bayerite during carbonation process under Expt 1, 2, 4 and 5. The growth rate of bayerite is always several orders of magnitude higher than that of gibbsite, which indicates that growth of bayerite is kinetically favored.

Supplementary references:

1. P. Sipos, G. Hefter and P. M. May, *Talanta*, 2006, **70**, 761.

2. R. J. Moolenaar, J. C. Evans and L. McKeever, *J. Phys. Chem.*, 1970, **74**, 3629.